Abstinence-dependent dissociable central amygdala microcircuits control drug craving

Marco Venniro[a,1], Trinity I. Russell[a], Leslie A. Ramsey[a], Christopher T. Richie[b], Heidi M. B. Lesscher[c], Simone M. Giovanetti[d,e], Robert O. Messing[d,e], and Yavin Shaham[a,1]

[a]Behavioral Neuroscience Branch Intramural Research Program, National Institute on Drug Abuse (NIDA), NIH, Baltimore, MD 21224; [b]Genetic Engineering and Viral Vector Core Intramural Research Program, NIDA, NIH, Baltimore, MD 21224; [c]Department of Animals in Science and Society, Utrecht University, 3584 CM, Utrecht, The Netherlands; [d]Department of Neurology, The University of Texas at Austin, Austin, TX 78712; and [e]Department of Neuroscience, The University of Texas at Austin, Austin, TX 78712

Edited by Huda Akil, University of Michigan–Ann Arbor, Ann Arbor, MI, and approved February 25, 2020 (received for review January 28, 2020)

We recently reported that social choice-induced voluntary abstinence prevents incubation of methamphetamine craving in rats. This inhibitory effect was associated with activation of protein kinase-Cδ (PKCδ)-expressing neurons in central amygdala lateral division (CeL). In contrast, incubation of craving after forced abstinence was associated with activation of CeL-expressing somatostatin (SOM) neurons. Here we determined the causal role of CeL PKCδ and SOM in incubation using short-hairpin RNAs against PKCδ or SOM that we developed and validated. We injected two groups with shPKCδ or shCtrl$_{PKCδ}$ into CeL and trained them to lever press for social interaction (6 d) and then for methamphetamine infusions (12 d). We injected two other groups with shSOM or shCtrl$_{SOM}$ into CeL and trained them to lever press for methamphetamine infusions (12 d). We then assessed relapse to methamphetamine seeking after 1 and 15 abstinence days. Between tests, the rats underwent either social choice-induced abstinence (shPKCδ groups) or homecage forced abstinence (shSOM groups). After test day 15, we assessed PKCδ and SOM, Fos, and double-labeled expression in CeL and central amygdala medial division (CeM). shPKCδ CeL injections decreased Fos in CeL PKCδ-expressing neurons, increased Fos in CeM output neurons, and reversed the inhibitory effect of social choice-induced abstinence on incubated drug seeking on day 15. In contrast, shSOM CeL injections decreased Fos in CeL SOM-expressing neurons, decreased Fos in CeM output neurons, and decreased incubated drug seeking after 15 forced abstinence days. Our results identify dissociable central amygdala mechanisms of abstinence-dependent expression or inhibition of incubation of craving.

social reward | amygdala | PKCδ | SOM | voluntary abstinence

Social factors play a critical role in human addiction (1). Negative social interaction promotes drug use and relapse (2), while positive social interaction has opposite effects (3, 4). This knowledge, together with early evidence for a role of classical and operant conditioning in addiction (5–7), led to the development of the community reinforcement approach (8) and, more recently, the therapeutic workplace (9, 10). The goal of these conditioning- and choice-based behavioral treatments is to substitute drug use with alternative nondrug social rewards (e.g., family support and employment) contingent, at least in part, on cessation of or decrease in drug use (3, 8). The neurobiological mechanisms underlying the protective effect of volitional positive social interaction on drug use and relapse are largely unknown, and this important facet of human addiction has not been incorporated into modern neuroscience investigation using preclinical addiction models (1, 11).

To address this research gap, we recently developed an operant-based rat community reinforcement model in which drug-experienced rats can choose between intravenous (i.v.) drug injections and social interaction with their peers (12–14). We found that the availability of a mutually exclusive operant social reward eliminated methamphetamine, heroin, and remifentanil self-administration (12–14), even in rats that met criteria for addiction (15). This protective effect persisted in socially housed rats and occurred independent of the rats' self-administration history (social self-administration training before or after drug self-administration) (12). Additionally, social choice-induced voluntary abstinence (termed herein voluntary abstinence) decreased incubation of heroin craving (13) and prevented incubation of methamphetamine craving (12). Incubation of craving refers to the time-dependent increase in drug seeking that occurs after forced abstinence in the homecage (16–18).

Previous studies using transgenic Cre-driver lines of mice demonstrated that protein kinase-Cδ (PKCδ)-expressing neurons in central amygdala (CeA) lateral subdivision (CeL) inhibit output neurons in central amygdala medial subdivision (CeM) that promote aversive behavior (fear conditioning), while CeL Somatostatin (SOM)-expressing neurons promote motivated behavior (either aversive or appetitive) by disinhibition of CeM output neurons (19–25). These studies parallel our initial investigation of mechanisms underlying the inhibitory effect of operant social reward on incubation of methamphetamine craving, where we found that this effect was associated with activation (indexed by the neuronal activity marker Fos) of PKCδ-expressing neurons in CeL and inhibition of CeM output neurons. In contrast, we found

Significance

Social support promotes drug abstinence. We incorporated this cardinal feature in our community-reinforcement model using rewarding social interaction. We found that social choice-induced abstinence prevented incubation of methamphetamine craving, an effect associated with activation of PKCδ-expressing neurons in CeL and inhibition of CeM neurons. In contrast, incubation after forced abstinence was associated with activation of CeL SOM-expressing neurons and CeM neurons. Here, using novel short-hairpin RNAs, we showed that the inhibitory effect of social interaction on incubation was mediated by activation of CeL PKCδ, leading to inhibition of CeM neurons. In contrast, incubation after forced abstinence was mediated by activation of CeL SOM, leading to activation of CeM neurons. Dissociable central amygdala mechanisms mediate abstinence-dependent expression or inhibition of craving.

Author contributions: M.V., L.A.R., R.O.M., and Y.S. designed research; M.V., T.I.R., L.A.R., C.T.R., H.M.B.L., S.M.G., R.O.M., and Y.S. performed research; C.T.R., H.M.B.L., S.M.G., and R.O.M. contributed new reagents/analytic tools; M.V., L.A.R., C.T.R., and Y.S. analyzed data; and M.V., T.I.R., L.A.R., C.T.R., H.M.B.L., S.M.G., R.O.M., and Y.S. wrote the paper.

The authors declare no competing interest.

This article is a PNAS Direct Submission.

Published under the PNAS license.

[1]To whom correspondence may be addressed. Email: venniro.marco@nih.gov or yshaham@intra.nida.nih.gov.

This article contains supporting information online at https://www.pnas.org/lookup/suppl/doi:10.1073/pnas.2001615117/-/DCSupplemental.

First published March 23, 2020.

Downloaded by guest on November 3, 2020

that after forced abstinence, incubation of methamphetamine craving was associated with activation of both CeL SOM-expressing neurons and CeM output neurons (12).

However, since results from studies using Fos or other activity markers are correlational, it is unknown whether activation of CeL PKCδ neurons after voluntary abstinence plays a causal role in the inhibition of incubation. Likewise, it is unknown whether activation of CeL SOM neurons after forced abstinence is the cause or the consequence of incubation of drug craving. At present, transgenic rat Cre-driver lines that would allow us to inhibit the activity of CeL PKCδ- and SOM-expressing neurons and study their causal role in incubation of craving do not yet exist. Moreover, in the abovementioned studies of CeL neuronal subpopulations, PKCδ and SOM have been used only as anatomical markers without exploration of their functional role in behavior.

In the present study, we took an alternative approach and examined the causal role of CeL PKCδ in preventing incubation of methamphetamine craving after voluntary abstinence and CeL SOM in promoting incubation of craving after forced abstinence. For this purpose, we decreased the levels of PKCδ and SOM by RNA interference using novel short-hairpin RNAs (shRNAs) that we validated first in vitro and then evaluated by immunohistochemistry and ex vivo brain slice electrophysiology. Surprisingly, these shRNAs potently decreased neuronal activity of CeL neurons in a cell type-specific manner. We then used them to test the causal role of CeL PKCδ and SOM neurons in the abstinence-dependent modulation of incubation of methamphetamine craving.

We showed that shPKCδ CeL injections decreased Fos expression in CeL PKCδ neurons, increased Fos expression in CeM output neurons, and reversed the inhibitory effect of voluntary abstinence on incubation of drug craving. In contrast, shSOM CeL injections decreased Fos expression in CeL SOM neurons, decreased Fos expression in CeM output neurons, and decreased incubation of drug craving after forced abstinence. Our results identify dissociable central amygdala cellular mechanisms that regulate the abstinence-dependent inhibition and expression of incubation of craving.

Results

In the experiments described below, we investigated the causal role of CeL PKCδ and SOM in incubation of methamphetamine seeking after either voluntary abstinence or forced abstinence. First, in experiment 1, we developed short-hairpin RNAs to selectively knock down PKCδ and SOM by RNA interference (*SI Appendix*, Figs. S1 and S2) and validated their effectiveness in cultured cell lines. Second, we validated their efficacy in rat brains by injecting the AAV viruses encoding the shRNAs constructs (and their controls; *SI Appendix*, Fig. S3) using immunohistochemistry (after novel context-induced Fos expression) and ex vivo whole-cell clamp electrophysiology. In experiment 2, we tested whether incubation of methamphetamine craving after voluntary abstinence would be restored by knocking down CeL-PKCδ, resulting in increased activity of CeM output neurons. In experiment 3, we tested whether incubation of methamphetamine craving after forced abstinence would be decreased by knocking down CeL-SOM, resulting in decreased activity CeM output neurons.

Development and Validation of shPKCδ and shSOM Viruses. We initially developed short-hairpin RNAs to selectively knock down PKCδ and SOM by RNA interference. We first validated the effectiveness of these shRNAs in cultured cell lines (*SI Appendix*, Figs. S1 and S2). For PKCδ, we tested two different constructs (shPKCδ 4-1 and shPKCδ 2-1; *SI Appendix*, Fig. S1), and only the sh4-1 sequence is conserved in the rat. Therefore, this is the sequence we chose to move forward into AAV viral vectors expressing a Nuc-eYFP reporter. We tested the AAVs viruses encoding $shCtrl_{PKCδ}$ or shPKCδ in vitro using primary cortical neurons that use epifluorescence for Nuc-eYFP detection (*SI Appendix*, Fig. S3*A*). For SOM, we tested three different constructs (shSOM1, shSOM2, and shSOM3; *SI Appendix*, Fig. S2), and based on our data we moved shSOM2 into AAV viral vectors expressing a Nuc-eYFP reporter. We tested the AAVs viruses encoding $shCtrl_{SOM}$ or shSOM in vitro using primary cortical neurons that use epifluorescence for Nuc-eYFP detection (*SI Appendix*, Fig. S3*B*).

In experiment 1A, we used immunohistochemistry to validate their efficacy in rat brain following viral delivery by injecting $shCtrl_{PKCδ}$ or shPKCδ (n = 6; within-subjects design) into the CeL (0.75 μL) either 2 or 4 wk before novel context exposure. We injected each rat with $shCtrl_{PKCδ}$ in one hemisphere and shPKCδ in the other hemisphere (counterbalanced). On test day, we placed the rats into a novel context (spherical container with fresh bedding and colorful toys) to induce Fos expression, and 90 min later we collected tissue for viral expression and Fos, PKCδ, and Fos + PKCδ double-labeling in CeL. We found that CeL shPKCδ injections significantly decreased CeL PKCδ levels (paired t test, $t_5 = 6.1$, $P = 0.002$); these injections also modestly decreased Fos and Fos + PKCδ expression, but these effects did not reach statistical significance (paired t test, $t_5 = 2.1$ and 2.2, $P = 0.086$ and 0.081) (Fig. 1 *A* and *B* and *SI Appendix*, Table S1, for statistical results). We determined the distribution of viral expression by the presence of GFP immunoreactivity (*SI Appendix*, Fig. S4*A*). Because shPKCδ modestly reduced Fos expression, we hypothesized that PKCδ knockdown would reduce the excitability of CeL PKCδ neurons. To test this hypothesis, we performed whole-cell current clamp recordings in CeL and examined the effect of shPKCδ on intrinsic excitability (Fig. 1*C*). CeL neurons expressing shPKCδ showed reduced firing in response to depolarizing current injections compared with CeL neurons expressing the $shCtrl_{PKCδ}$. The analysis showed a Current x shRNA type interaction ($F_{19,247} = 4.37$, $P < 0.001$). There was no difference in resting membrane potential between the two groups ($P > 0.05$).

In experiment 1B, we similarly validated the shSOM virus. We bilaterally injected the $shCtrl_{SOM}$ or shSOM viruses (n = 5 per group, between-subjects design) into CeL (0.375 μL) 4 wk before novel context exposure. Using immunohistochemistry, we found that shSOM but not $shCtrl_{SOM}$ decreased CeL SOM levels (unpaired t test, $t_8 = 5.4$, $P = 0.001$) and Fos expression ($t_8 = 5.1$, $P = 0.001$) but not Fos + SOM ($t_8 = 1.9$, $P = 0.10$) (Fig. 1 *D* and *E*). We determined the distribution of viral expression by the presence of GFP immunoreactivity (*SI Appendix*, Fig. S4*C*). Since shSOM reduced Fos expression, we hypothesized that SOM knockdown would reduce the excitability of CeL SOM neurons. To test this possibility, we performed whole-cell current clamp recordings in CeL SOM neurons to examine the effect of shSOM on intrinsic excitability (Fig. 1*F*). CeL neurons expressing shSOM showed reduced firing in response to depolarizing current injections compared with CeL neurons expressing $shCtrl_{SOM}$. The analysis showed a main effect of shRNA type ($F_{1,13} = 7.03$, $P = 0.02$). Additionally, at rest, CeL shSOM neurons were more hyperpolarized than $shCtrl_{SOM}$ neurons ($t_{11} = 3.5$, $P = 0.005$).

CeL PKCδ Knockdown Reversed the Inhibitory Effect of Voluntary Abstinence on Incubation of Craving. We previously showed that the inhibitory effect of voluntary abstinence on incubation of methamphetamine craving is associated with increased Fos expression in CeL PKCδ neurons and reduced Fos expression in CeM output neurons (12). In experiment 2, we investigated whether CeL PKCδ mediates this inhibitory effect. The experiment consisted of three phases (Fig. 2*A*): social self-administration training (6 d, 60 s interaction) followed by CeL $shCtrl_{PKCδ}$ or shPKCδ injections, methamphetamine self-administration (12 d, 6 h/d, 0.1 mg/kg/infusion), and relapse tests 1 d (30-min session) after

NEUROSCIENCE

Downloaded by guest on November 3, 2020

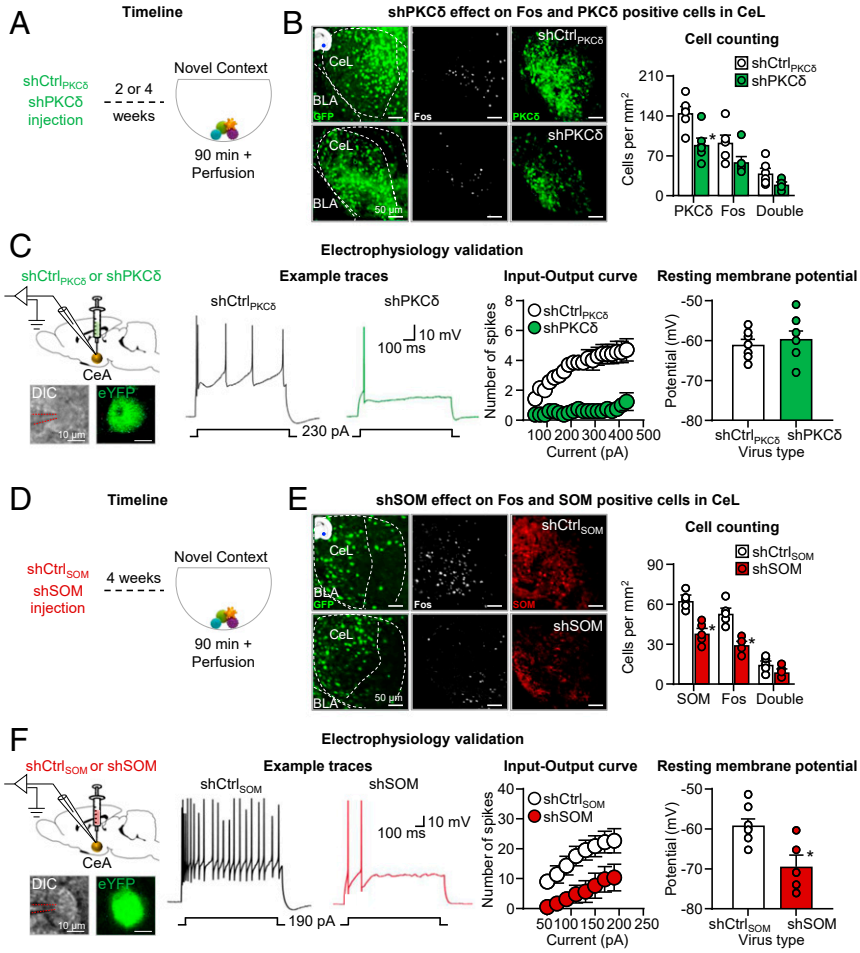

Fig. 1. *shPKCδ and shSOM validation.* (*A*) Timeline of the experiment (shPKCδ). We injected six male rats with $shCtrl_{PKCδ}$ into the CeL of one hemisphere and shPKCδ into the other hemisphere (counterbalanced) either 2 or 4 wk prior to novel context-induced Fos expression. (*B*) shPKCδ effect on Fos expression and PKCδ levels in CeL. (*Left*) Representative CeL photomicrographs of $shCtrl_{PKCδ}$ (*Top*) and shPKCδ (*Bottom*) viral expression, Fos, and PKCδ expression ($n = 6$). Virus is shown in green, Fos is shown in white, and PKCδ is shown in green. (Scale bars, 50 μm.) (*Right*) Cell counting graph (reporting also individual data) for Fos, PKCδ, and double-labeled neurons. (*C*). Electrophysiology validation. The first panel shows a representative photomicrograph of recorded cells. (Scale bars, 10 μm.) The second panel shows example traces showing spiking activity in response to a depolarizing somatic current injection in CeL neurons expressing either $shCtrl_{PKCδ}$ or shPKCδ. The third panel shows input–output curve demonstrating spiking activity output in response to depolarizing steps of current input in CeL neurons expressing either $shCtrl_{PKCδ}$ or shPKCδ. The fourth panel shows summary data showing resting membrane potential of recorded CeL neurons expressing either $shCtrl_{PKCδ}$ or shPKCδ. (*D*) Timeline of the experiment (SOM). We injected two groups of male rats ($n = 5$) bilaterally with $shCtrl_{SOM}$ or shSOM into the CeL 4 wk prior to novel context-induced Fos expression. (*E*) shSOM effect on Fos expression and SOM levels in CeL. (*Left*) Representative CeL photomicrographs of $shCtrl_{SOM}$ (*Top*) and shSOM (*Bottom*) viral expression and Fos and SOM expression ($n = 5$ per group). Virus is shown in green, Fos is shown in white, and SOM is shown in red. (Scale bars, 50 μm.) (*Right*) Cell counting graph (reporting also individual data) for Fos, SOM, and double-labeled neurons. (*F*). Electrophysiology validation. The first panel shows a representative photomicrograph of recorded cells. (Scale bars, 10 μm.) The second panel shows example traces showing spiking activity in response to a depolarizing somatic current injection in CeL neurons expressing either $shCtrl_{SOM}$ or shSOM. The third panel shows input–output curve demonstrating spiking activity output in response to depolarizing steps of current input in CeL neurons expressing either $shCtrl_{SOM}$ or shSOM. The fourth panel shows a summary graph showing resting membrane potential of recorded CeL neurons expressing either $shCtrl_{SOM}$ or shSOM. *, different from shCtrl control viruses, $P < 0.05$. See also *SI Appendix*, Figs. S1–S3. Statistical details are included in *SI Appendix*, Table S1.

the last self-administration session and after 15 d (90-min session) of voluntary abstinence.

Training and voluntary abstinence. The rats increased the number of social and methamphetamine rewards during training, and there were no group differences during this phase (Fig. 2*B* and *SI Appendix*, Table S1, for statistical results). CeL $shCtrl_{PKCδ}$, and shPKCδ injections had no effect on the rats' strong preferences for social reward over methamphetamine (Fig. 2*C*). The analysis of the preference score showed a significant effect of session ($F_{9,189} = 5.0$, $P < 0.001$), but not shRNA type or session × shRNA type interaction (P values > 0.05).

Relapse tests. The results of the 30-min day 1 test and the first 30 min of day 15 test showed that the rats in the shPKCδ but not $shCtrl_{PKCδ}$ condition sought methamphetamine more on abstinence day 15 than on day 1 (Fig. 2*D*). The statistical analysis, which included the between-subjects factor of shRNA type ($shCtrl_{PKCδ}$ or shPKCδ) and the within-subjects factors of abstinence day (1, 15) and lever (active or inactive) showed a significant interaction between the three factors ($F_{1,21} = 4.3$, $P = 0.050$). We also analyzed the data from the 90-min day 15 relapse test session using the factors of shRNA type and session minute (30, 60, and 90 min) (*SI Appendix*, Fig. S5*A*). This analysis showed significant interaction between the two factors ($F_{2,42} = 3.7$, $P = 0.032$). These results indicate that shPKCδ but not $shCtrl_{PKCδ}$ increased the response to the methamphetamine cues during the first 30 min of testing but had no effect on within-session

Downloaded by guest on November 3, 2020

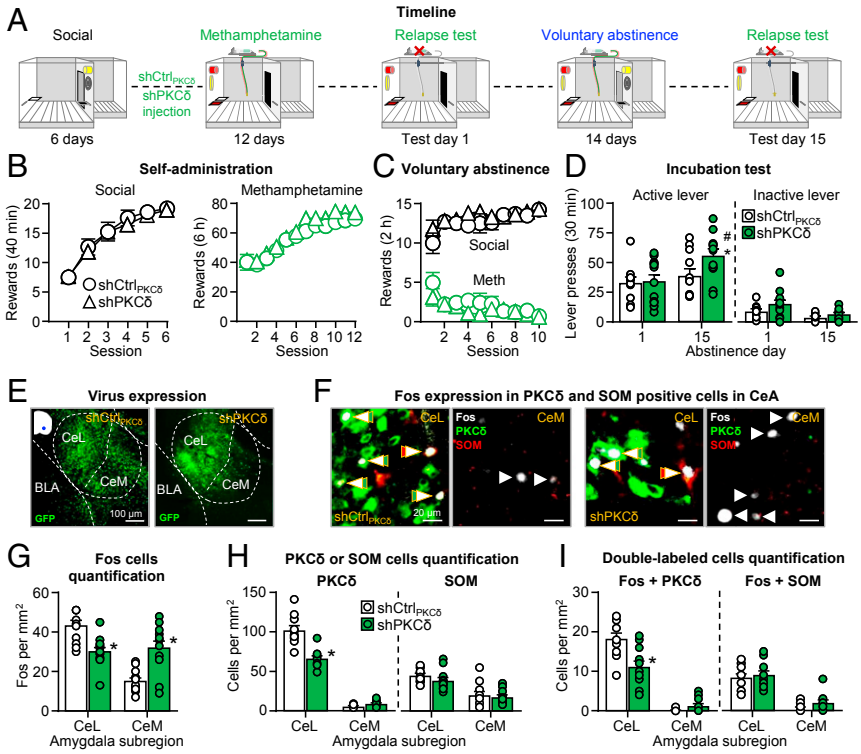

Fig. 2. CeL shPKCδ virus injections reversed the inhibitory effect of voluntary abstinence on incubation of methamphetamine craving. (*A*) Timeline of the experiment. (*B*) Self-administration training (rewards: social or methamphetamine infusion). Number of social rewards (20 trials) or methamphetamine infusions (6 h). (*C*) Voluntary abstinence. Social rewards and methamphetamine infusions earned during 10 discrete choice sessions (15 trials per session). (*D*) Incubation test. (*Left*) Active lever and (*Right*) inactive lever presses during the 30-min test sessions (including individual data). During testing, active lever presses led to contingent presentation of the discrete light cue previously paired with methamphetamine infusions during training but not methamphetamine (extinction conditions). $shCtrl_{PKCδ}$ $n = 11$; shPKCδ $n = 12$ male rats. *, different from test day 1 within each shRNA type, $P < 0.05$; #, different from $shCtrl_{PKCδ}$ on day 15, $P < 0.05$. Data are mean ± SEM. (*E*) Virus expression. Representative CeA photomicrographs of $shCtrl_{PKCδ}$ (*Left*) and shPKCδ (*Right*) viral expression (green). (Scale bars, 100 μm.) (*F*) Representative CeL and CeM photomicrographs of Fos expression in PKCδ and SOM neurons: (*Left*) $shCtrl_{PKCδ}$ group ($n = 11$) and (*Right*) shPKCδ group ($n = 12$). Arrows indicate representative cells; double arrows indicate double-labeled cells. Fos is shown in white, PKCδ is shown in green, and SOM is shown in red. (Scale bars, 20 μm.) (*G*) Fos neuron quantification. Number of Fos-immunoreactive (IR) neurons per mm^2 in the CeL and CeM. (*H*) PKCδ and SOM quantification. Number of PKCδ-IR or SOM-IR in CeL and CeM. (*I*) Quantification of double-labeled cells. Number of Fos + PKCδ-IR or Fos + SOM-IR double-labeled neurons per mm^2 in the CeL and CeM. *, different from $shCtrl_{PKCδ}$, $P < 0.05$. Data are mean ± SEM. See also *SI Appendix*, Figs. S1, S3, and S4.

extinction learning. We report the extent of viral expression for these experiments in *SI Appendix*, Fig. S4*B*.

Immunohistochemistry. After the 90-min day 15 relapse test, we first assessed virus expression (Fig. 2*E*). We then analyzed Fos expression, PKCδ and SOM protein levels, and double-labeled Fos + PKCδ and Fos + SOM (Fig. 2 *F*–*I*). For Fos, CeL shPKCδ injections decreased Fos in CeL and increased Fos in CeM (Fig. 2 *F* and *G*). The statistical analysis showed a significant interaction of shRNA type × amygdala subregion (CeL, CeM) ($F_{1,21} = 44.4$, $P < 0.001$). For PKCδ, CeL shPKCδ injections decreased PKCδ protein levels in CeL but not CeM (Fig. 2 *F* and *H*), as indicated by a shRNA type × amygdala subregion interaction ($F_{1,21} = 39.8$, $P < 0.001$). For SOM, CeL shPKCδ injections had no effect on SOM protein levels in either CeL or CeM (P values > 0.05) (Fig. 2 *F* and *H*). For Fos + PKCδ double-labeling, CeL shPKCδ injections decreased Fos in PKCδ neurons in CeL but not CeM, as indicated by a significant shRNA type × amygdala subregion interaction ($F_{1,21} = 26.9$, $P < 0.001$) (Fig. 2 *F* and *I*). For Fos + SOM double-labeling, CeL shPKCδ injections had no effect on Fos expression in SOM neurons in CeL or CeM. The statistical analysis showed a main effect of amygdala subregion ($F_{1,21} = 92.1$, $P < 0.001$), reflecting higher expression of Fos + SOM in CeL but no effects of shRNA type or interaction between the two factors (P values > 0.05) (Fig. 2 *F* and *I*).

Taken together, in agreement with our previous findings (12), voluntary abstinence prevented incubation of craving in rats injected with the $shCtrl_{PKCδ}$ control virus. More importantly, knockdown of PKCδ in the CeL with shPKCδ reversed the inhibitory effect of voluntary abstinence on incubation of methamphetamine craving by decreasing the activity of CeL PKCδ neurons and increasing the activity of CeM output neurons.

CeL SOM Knockdown Decreased Incubation of Methamphetamine Craving after Forced Abstinence. We previously showed that incubation of methamphetamine craving after forced abstinence was associated with increased Fos expression in CeL SOM neurons and increased Fos expression in CeM output neurons (12). In experiment 3, we determined whether decreasing CeL SOM levels will decrease incubation of methamphetamine craving after forced abstinence. The experiment consisted of two phases (Fig. 3*A*): CeL $shCtrl_{SOM}$ or shSOM injections, followed by methamphetamine self-administration (12 d, 6 h/d, 0.1 mg/kg/infusion) and relapse tests 1 d (30-min session) after the last self-administration session and after 15 d (90-min session) of forced abstinence.

Training. The rats increased the number of methamphetamine infusions during training, and there were no group differences during this phase (Fig. 3*B* and *SI Appendix*, Table S1, for statistical results) (P values > 0.05).

NEUROSCIENCE

Downloaded by guest on November 3, 2020

Relapse tests. The results of the 30-min day 1 test and the first 30 min of day 15 test showed that the rats in the $shCtrl_{SOM}$ but not shSOM condition sought methamphetamine more on abstinence day 15 than on day 1 (Fig. 3*C*). The statistical analysis showed a significant shRNA type × abstinence day interaction ($F_{1,24} = 13.0$, $P = 0.001$). We also analyzed the data from the 90-min day 15 relapse test session using the factors of shRNA type and session minute (*SI Appendix*, Fig. S5*B*). This analysis showed significant interaction between the two factors ($F_{2,48} = 10.7$, $P < 0.001$). These results indicate that shSOM but not $shCtrl_{SOM}$ decreased the response to the methamphetamine cues during the first 30 min of testing but had no effect on within-session extinction learning. We reported the extent of viral expression for these experiments in *SI Appendix*, Fig. S4*D*.

Immunohistochemistry. After the 90-min day 15 relapse test, we first assessed virus expression (Fig. 3*D*). We then analyzed Fos expression, PKCδ and SOM protein levels, and double-labeled Fos + PKCδ and Fos + SOM (Fig. 3 *E*–*H*). For Fos, CeL shSOM injections decreased Fos expression in both CeL and CeM (Fig. 3 *E* and *F*). The statistical analysis showed a main effect of shRNA type ($F_{1,24} = 10.05$, $P = 0.004$) but not of amygdala subregion or an interaction between the two factors (*P* values > 0.05). For PKCδ, CeL shSOM injections had no effect on PKCδ protein levels in either the CeL or CeM (*P* values > 0.05) (Fig. 3 *E* and *G*). For SOM, CeL shSOM injections decreased SOM protein levels in CeL but not CeM, as indicated by a significant interaction between shRNA type × amygdala subregion ($F_{1,24} = 15.4$, $P = 0.001$) (Fig. 3 *E* and *G*). For Fos + SOM double-labeling, CeL shSOM injections decreased Fos expression in SOM neurons in CeL but not CeM, as indicated by a significant shRNA type × amygdala subregion interaction ($F_{1,21} = 16.8$, $P < 0.001$) (Fig. 3 *E* and *H*). For Fos + PKCδ double-labeling, CeL shSOM injections had no effect on Fos + PKCδ double-labeling in CeL or CeM. The analysis showed a main effect of amygdala subregion ($F_{1,24} = 254.1$, $P < 0.001$), reflecting higher expression of Fos + PKCδ in CeL than in CeM, but no significant effects of shRNA type or an interaction between the two factors (*P* values > 0.05) (Fig. 3 *E* and *H*).

Taken together, knockdown of SOM in the CeL with shSOM decreased incubation of methamphetamine craving after forced abstinence by decreasing the activity of CeL SOM neurons and CeM output neurons.

Discussion

Our study identified CeL PKCδ and SOM neurons as critical components of dissociable central amygdala microcircuits controlling abstinence-dependent inhibition and expression of incubation of methamphetamine craving (Fig. 4). Our study also introduces two viral tools for studying the functional role of the PKCδ enzyme and the SOM peptide in different neuronal populations in multiple brain areas of nontransgenic rats and potentially other species.

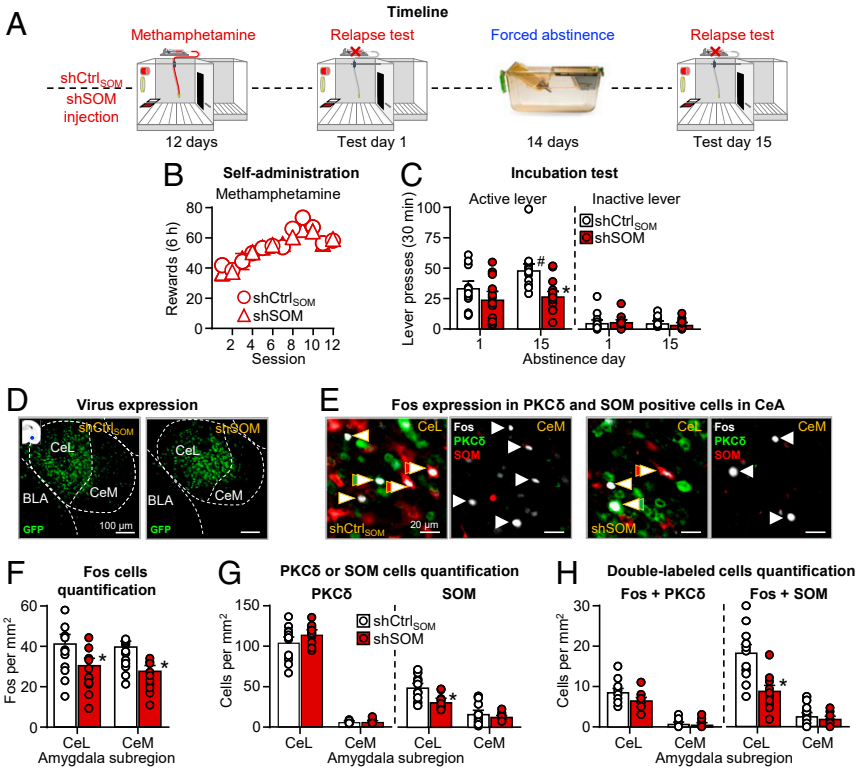

Fig. 3. CeL shSOM injections decreased incubation of methamphetamine craving after forced abstinence. (*A*) Timeline of the experiment. (*B*) Self-administration training (methamphetamine infusions). Number of methamphetamine infusions (6 h). (*C*) Incubation test. (*Left*) Active lever and (*Right*) inactive lever during the 30-min test sessions (including individual data). During testing, active lever presses led to contingent presentation of the discrete light cue previously paired with methamphetamine infusions during training but not methamphetamine (extinction conditions). $shCtrl_{SOM}$ $n = 13$; shSOM $n = 13$ male rats. #, different from test day 1 within each shRNA type; *, different from $shCtrl_{SOM}$ on day 15, $P < 0.05$. Data are mean ± SEM. (*D*) Virus expression. Representative CeA photomicrographs of $shCtrl_{SOM}$ (*Left*) and shSOM (*Right*) viral expression (green). (Scale bars, 100 μm.) (*E*) Representative CeL and CeM photomicrographs of Fos expression in PKCδ and SOM neurons: (*Left*) $shCtrl_{SOM}$ group ($n = 13$) and (*Right*) shSOM group ($n = 13$). Arrows indicate representative cells; double arrows indicate double-labeled cells. Fos is shown in white, PKCδ is shown in green, and SOM is shown in red. (Scale bars, 20 μm.) (*F*) Fos neuron quantification. Number of Fos-immunoreactive (IR) neurons per mm^2 in the CeL and CeM. (*G*) PKCδ and SOM quantification. Number of PKCδ-IR or SOM-IR in CeL and CeM. (*H*) Quantification of double-labeled cells. Number of Fos + PKCδ-IR or Fos + SOM-IR double-labeled neurons per mm^2 in the CeL and CeM. *, different from $shCtrl_{SOM}$, $P < 0.05$. Data are mean ± SEM. See also *SI Appendix*, Figs. S2–S4.

Downloaded by guest on November 3, 2020

We recently showed that the inhibitory effect of social reward on incubation of methamphetamine craving is correlated with increased Fos expression in CeL PKCδ neurons and reduced Fos expression in CeM output neurons. In contrast, incubation of methamphetamine craving after forced abstinence was correlated with increased Fos expression in both CeL SOM neurons and CeM neurons (12). Based on these correlational Fos expression data and studies on the functional heterogeneity of the CeL and CeM (19), we postulated that CeL PKCδ and SOM neurons play dissociable roles in incubation of drug craving after voluntary abstinence versus forced abstinence. Testing the involvement of central amygdala PKCδ or SOM in incubation of drug craving required the development of new tools to selectively inhibit PKCδ or SOM CeL neurons because the lack of transgenic rat Cre-lines prevents the use of optogenetic or chemogenetic modulators to selectively inhibit these cell types.

We found that shPKCδ CeL injections decreased neuronal activity in PKCδ neurons in CeL and increased activity of CeM output neurons, resulting in reversal of the inhibitory effect of voluntary abstinence induced by social choice on incubation of craving. In contrast, shSOM CeL injections decreased Fos expression in both CeL SOM neurons and CeM output neurons, resulting in inhibition of incubation of craving after forced abstinence in homecage. Our results are consistent with previous studies using transgenic mice showing that CeL PKCδ-expressing neurons inhibit CeM output neurons that promote aversive behaviors, while CeL SOM-expressing neurons promote aversive or appetitive behaviors by disinhibition of CeM output neurons (20–25).

However, direct long-range projections from CeL SOM neurons to downstream central amygdala targets like bed nucleus of stria terminalis and periaqueductal gray contribute to aversive motivated behaviors (26, 27) and potentially appetitive behaviors as well (28). Therefore, the inhibitory effect of CeL shSOM injections on incubation after forced abstinence could be due to the inhibitory effect of these injections on activity of these motivationally relevant long-range projections. Additional evidence for the bidirectional nature of CeL PKCδ and SOM neurons is their opposite roles in pain modulation: activation of CeL PKCδ neurons increases pain, while activation of CeL SOM neurons decreases pain (29).

Our results expand our understanding of the role of CeL PKCδ and SOM neurons in motivated behaviors. Previous mouse transgenic studies established a role of PKCδ- and SOM-expressing neurons in different behaviors. In contrast, the current findings establish a causal role of the PKCδ and the SOM in the CeL in motivated behavior. An unexpected finding was that our viral constructs not only decreased the levels of PKCδ and the SOM but also potently decreased neuronal activity in a cell type-specific manner. Based on the previous literature described above, this inhibitory effect on cell activity likely mediates the effects of the viral manipulations on incubation of drug craving.

In conclusion, we identified abstinence-dependent, cell type-specific, central amygdala microcircuit mechanisms that bidirectionally control incubation of methamphetamine craving after either voluntary abstinence or forced abstinence. Our results expand our understanding of the critical role of central amygdala in incubation of drug craving after forced abstinence (17, 18, 30, 31), relapse after food choice-induced voluntary abstinence (32), and the incentive motivational effects of drug and nondrug rewards (33, 34). Finally, it is well established that exposure to drug-associated cues increases amygdala activity in human drug users (35, 36). Additionally, human imaging studies reported that in drug users, changes in resting-state functional connectivity of amygdala-related circuits are associated with relapse risk (37, 38). We hope that our study will inspire clinical studies to determine whether social-based treatment approaches like the community reinforcement approach (8) and the therapeutic workplace (9) will restore normal amygdala function, resulting in reduced long-term relapse risk.

Materials and Methods

Subjects. We used male Sprague–Dawley rats (Charles River, $n = 108$; 36 social partners) weighing 150 to 175 g upon arrival. For experiments 1A and 1B, we housed rats two per cage. For experiments 2 and 3, we housed rats two per cage for 2 to 3 wk and then individually housed them for the duration of the experiment starting 1 wk prior to either social (experiment 2) or methamphetamine (experiment 3) self-administration. In experiment 2, we randomly assigned the rats to the "resident (drug user)" and "social partner (drug naïve)" groups. We maintained all rats on a reverse 12-h light/dark cycle (lights off at 9:30 AM) with free access to standard laboratory chow and water. Our procedures followed the guidelines outlined in the Guide for the Care and Use of Laboratory Animals (39). Our study was approved by the NIDA Intramural Research Program Animal Care and Use Committee. We excluded 23 rats due to sickness ($n = 3$) or viruses' misplacement ($n = 20$).

Surgery. We performed all surgeries before methamphetamine self-administration training. We anesthetized the rats with isoflurane (5% induction; 2 to 3% maintenance) and injected ketoprofen (2.5 mg/kg, s.c. Butler Schein) after surgery and the following day to relieve pain and decrease inflammation. We allowed the rats to recover from surgery for 4 to 5 d before training.

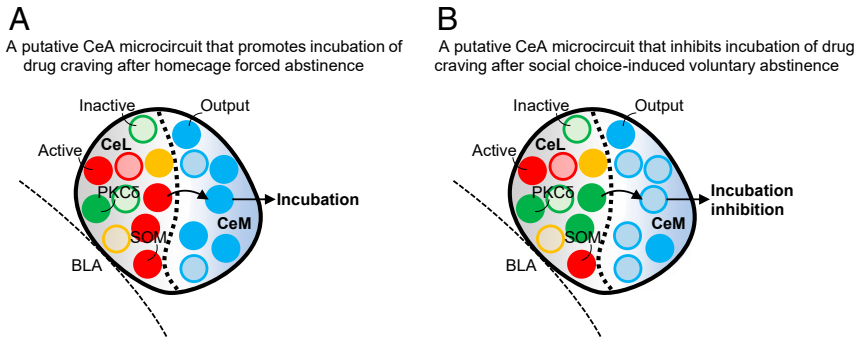

Fig. 4. Schematic illustration of the dissociable CeA mechanisms mediating abstinence-dependent expression or inhibition of incubation of methamphetamine craving. (*A*) A putative central amygdala microcircuit that promotes incubation of drug craving after forced abstinence: active CeL somatostatin (SOM) neurons activate CeM output neurons (via disinhibition) and promote incubation. (*B*) A putative central amygdala microcircuit that inhibits incubation of drug craving after voluntary abstinence: active CeL PKCδ neurons inhibit CeM output neurons and inhibit incubation. CeL, CeM, central amygdala lateral and medial subdivision; BLA, basolateral amygdala. Full circle indicates active neurons, and empty circle indicates inactive neurons. PKCδ neurons (green), SOM neurons (red), output neurons (blue) neurons, and other neurons (yellow).

Downloaded by guest on November 3, 2020

I.V. Catheterization. We inserted Silastic catheters into the jugular vein, which passed s.c. to the midscapular region and attached to a modified 22-gauge cannula cemented to polypropylene mesh (Sefar). We flushed the catheters daily with sterile saline containing gentamicin (4.25 mg/mL; APP Pharmaceuticals) during the experiments.

Viral Injections. We injected viruses to selectively knockdown either PKCδ or SOM in CeL. We set the nose bar at −3.3 mm and used the following coordinates from Bregma (40), based on pilots and previous studies (30, 32): anterior-posterior (AP), −2.5 mm; medial-lateral (ML), ± 4.5 mm; dorsal-ventral (DV), −8.5 mm. We injected either 0.75 μL (experiments 1A and 2) or 0.375 μL (experiments 1B and 3) of virus in CeA over 5 min and left the needle in place for 5 min. We used 10 mL Nanofil syringes (World Precision Instruments) with 33-gauge needles, attached to an UltraMicroPump (UMP3) with SYS-Micro4 Controller (World Precision Instruments). We used different virus volumes to limit shSOM spread to the CeM. In experiments 1A (unilateral counterbalance) and 2 (bilateral), we used either $shCtrl_{PKCδ}$ (scAAV1-shCtrl-CMV-IE-Nuc-eYFP; Titer: 3.24E + 12 vg/mL) or shPKCδ (scAAV1-shPKCδ-CMV-IE-Nuc-eYFP; Titer: 2.56E + 12 vg/mL). In experiments 1B and 3 (both bilateral), we used either $shCtrl_{SOM}$ (AAV1-SYN1-Nuc-eYFP-miR-30a-(shCtrl); Titer: 2.1E + 10 vg/mL) or shSOM (AAV1-SYN-Nuc-eyFP-miR30a-(shSOM); Titer: 2.1E + 10 vg/mL).

Viral Vector Plasmid Construction.

shPKCδ. We designed short hairpin RNAs (shRNAs) from the sequence for mouse PKCδ mRNA (NCBI Accession No. NM_011103.3) using an siRNA selection program from the Whitehead Institute. The 19-nucleotide sequences we identified targeting mouse PKCδ were sh4-1, GGACAAAGGCCGCTTCGAA, and sh2-1, GGTGTTGATTGACGATGAT. Only the sh4-1 sequence is conserved in the rat, and this is the one we used for the experiment described below. As a control we used a sequence, GCGCTTAGCTGTAGGATTC, which does not align with any known mammalian gene in a BLAST search. We designed a stem-loop structure incorporating the 19-nucleotide target sequence (41) and synthesized complementary oligonucleotides encoding PKCδ shRNAs (Operon); next we annealed and cloned the construct into the lentiviral expression vector pLL3.7 (42).

We produced the lentivirus using a Virapower Kit (Invitrogen). Viral titers that we determined by p24 ELISA (Zeptometrix) were $\sim 8 \times 10^7$ pg/mL for all viruses. We determined knockdown efficiency by infection of mouse L-M(TK-) cells with lentivirus at 1 pg of p24 antigen per cell (∼1 infectious unit). We determined PKCδ protein levels by Western blot analysis using a goat anti-PKCδ antibody (Santa Cruz Biotechnology, 1:1,000 to 1,500 dilution; RRID:AB_670776) followed by goat anti-rabbit-peroxidase (Chemicon; 1:1,000 dilution; RRID:AB_390191) and visualized protein bands by enhanced chemiluminescence (Pierce Biotechnology). We scanned images of blots and calculated the optical density of each immunoreactive band using Fiji. We measured the amount of immunoreactivity in each sample as the slope of the line determined by optical density values measured at four different protein amounts (2.5, 5, 7.5, and 10 μg).

shSOM. We used the program shRNA Retriever maintained by Ravi Sachidanandam at Icahn School of Medicine, NY, to identify three shRNA sequences targeting the 3′UTR of somatostatin (SOM) into the vector pPRIME-GFP (Addgene no. 11657). We validated these shRNAs in HEK293 cells plated at a density of 3×10^5 cells per well in 12-well plates. The next day we cotransfected cells with an shSOM vector and a transgene encoding somatostatin with its 3′-UTR using Lipofectamine 2000 (Invitrogen). Seventy-two h after transfection, we extracted RNA using RNeasy Lipid Tissue Mini Kit (QIAGEN), reverse transcribed RNA samples using the High Capacity cDNA Synthesis Kit (Invitrogen), and determined knockdown efficiency by qPCR using GUSB mRNA for normalization. We performed qPCR using a TaqMan Gene Expression Assay Kit (Applied Biosystems) with probes for SOM (Rn00561967_m1) and GUSB (Hs00939627_m1), using a ViiA 7 Real-Time PCR System (Applied Biosystems).

We tested three different constructs (shSOM1, shSOM2, and shSOM3), and based on our data we used shSOM2 for the experiment described below. As a control we used the GCCGCGATTAGGCTGTTATAA sequence (43, 44) (Addgene no. 71384). We normalized SOM gene expression to the GUSB control sample.

AAV Packaging Vectors to shRNAs Delivery.

shPKCδ. We amplified the expression cassettes for the shRNAs driven by the murine U6 promoter from the pLL3.7 backbones by PCR and used to replace the MluI restriction fragment containing the Nluc shRNA cassette of pscAAV-mU6-shRNA(Nluc)-CMV-IE-Nuc-eYFP [Addgene no. 104986 (45)] using ligation-independent cloning. This resulted in pscAAV-shCtrl-CMV-IE-Nuc-eYFP ($shCtrl_{PKCδ}$; Addgene no. 135563) and pscAAV-shPKCδ-CMV-IE-Nuc-eYFP rat (shPKCδ; Addgene no. 135562). We verified the insert-containing clones by sequencing and restriction digest prior to packaging virus.

shSOM. We amplified the miR30a cassettes for the shRNAs by PCR and inserted downstream as a transcriptional fusion to the nuclear-localized eYFP reporter driven by the synapsin promoter in pAAV-SYN1-Nuc-EYFP (Addgene no. 135567), using ligation-independent cloning. We verified the insert-containing clones by sequencing and restriction digest prior to packaging virus. This resulted in pAAV-SYN1-Nuc-eYFP-miR-30a ($shCtrl_{SOM}$; Addgene no. 135564) and pAAV-SYN-Nuc-eYFP-miR30a (shSOM; Addgene no. 135565).

We packaged all four AAV plasmids as AAV1 serotype particles using triple transfection method as previously described (46). We titered the vectors by droplet digital PCR.

Drugs. We received (+)-methamphetamine-HCl (methamphetamine) dissolved in saline from the NIDA pharmacy. We used a unit dose of 0.1 mg/kg/infusion for self-administration training based on previous studies (12, 32, 47).

Immunohistochemistry. Immediately after the behavioral tests, we anesthetized the rats with isoflurane and perfused them transcardially with ∼100 mL of 0.1 M phosphate-buffered saline (PBS) (pH 7.4) followed by ∼400 mL of 4% paraformaldehyde (PFA) in PBS. We removed the brains and postfixed them in 4% PFA for 2 h before transferring them to 30% sucrose in PBS for 48 h at 4 °C. We froze the brains in dry ice and stored them at −80 °C. We cut coronal sections (40 μm) of the amygdala (AP bregma level of −1.92 to −2.76 mm) using a Leica cryostat. We collected the tissues in cryoprotectant (20% glycerol and 2% DMSO in 0.1 M PBS, pH 7.4) and stored them at −80 °C until further processing.

Viral injection site verification. We selected four series of sections of each rat and used immunofluorescence to determine viral injection sites. We repeatedly rinsed free-floating sections in PBS (3 × 10 min) and incubated them for 2 h in 0.5% PBS-Tx with 10% normal horse serum (NHS). We then incubated all sections for at least 48 h at 4 °C in chicken anti-GFP primary antibody (1:1,000; Aves Labs Inc., RRID: AB_2307313) diluted in 0.5% PBS-Tx with 2% NHS. After rinsing the sections in with PBS, we incubated them for 4 h in 0.5% PBS-Tx with 2% NHS and donkey anti-chicken Alexa Fluor 488 (1:500; Jackson ImmunoResearch, 703-545-155; RRID: AB_2340375). We then rinsed the sections in PBS, mounted them onto gelatin-coated glass slides, air-dried, and cover-slipped with antifade mounting medium (Vectashield).

Fos, PKCδ and SOM triple-labeling. We selected four series of sections of each rat and used immunofluorescence to double-label Fos with either PKCδ or SOM (experiment 1) or triple-label Fos with PKCδ and SOM (experiments 2 and 3). We used the same protocol described above, except that we used different antibodies. Primary antibodies were rabbit anti-Fos (1:1,000, Cell Signaling Technology, Phospho-c-Fos, 5348S; RRID: AB_10013220), mouse anti-PKCδ primary antibody (1:1,000, BD Biosciences, 610398, RRID:AB_397781), and rat anti-SOM (1:1,000, Millipore, MAB354, RRID:AB_2255365); secondary antibodies were donkey anti-rabbit Alexa Fluor 594 (1:500, Jackson Immuno Research, 711-585-152; RRID: AB_2340621), donkey anti-mouse DyLight Fluor 405 (1:500, Jackson Immuno Research, 715-475-150, RRID: AB_2340839), and donkey anti-rat Alexa Fluor 647 (1:500, Jackson Immuno Research, 712-605-153, RRID: AB_2340694).

Image acquisition and quantification. We used an ORCA-Flash 4.0 Digital camera (Hamamatsu, C11440-42U30) attached to a Zeiss Axio Scope Imager M2 using Micro-Manager 1.4 software (Open Imaging) to collect the images. We captured each image using a 10× (for viral placements) or 20× objective (for triple-labeling). We quantified the total number of Fos (white), PKCδ (green), and SOM (red) positive cells in CeL and CeM. For each rat, we quantified cells in two hemispheres of four sections, and we averaged the counts to give a mean number of each immunoreactive cell type. In the serial sections, we considered a cell immunopositive if it showed a neuron-like shape after we adjusted the pictures to match contrast and brightness using Fiji. We performed the image-based quantification in a blind manner. The mean interrater reliability (MV and TIR) for experiments 1A and 1B and experiments 2 and 3 were $r = 0.85$, 0.86, 0.85, and 0.81, $P < 0.05$. For viral injection site verification (*SI Appendix*, Fig. S4), we plotted each injection at 50% opacity so that overlap of injection sites is apparent with increased color intensity.

Ex Vivo Electrophysiology. We deeply anesthetized rats with isoflurane (60 to 90 s) and then rapidly removed their brains. We cut coronal sections (250 μm) containing the amygdala using a vibratome (Leica VT1000) in an ice-cold cutting solution containing (in mM) 92 NMDG, 20 Hepes, 25 glucose, 30 $NaHCO_3$, 1.2 NaH_2PO_4, 2.5 KCl, 5 Na-ascorbate, 3 Na-pyruvate, 2 thiourea, 10 $MgSO_4$, and 0.5 $CaCl_2$, saturated with 95% O_2, 5% CO_2, pH 7.3 to 7.4, 305 to 310 mOsm/kg. Slices recovered for a minimum of 30 min at 22 °C in artificial-CSF containing (in mM) 126 NaCl, 2.5 KCl, 1.2 $MgCl_2$, 2.4 $CaCl_2$, 1.2 NaH_2PO_4,

Downloaded by guest on November 3, 2020

21.4 $NaHCO_3$, 11.1 glucose, 3 Na-pyruvate, and 1 Na-ascorbate. We recorded at 32 to 35 °C in the same solution that was bath-perfused at 2 to 3 mL/min. The intracellular solution contained (in mM), 115 K-gluconate, 20 KCl, 1.5 $MgCl_2$, 10 Hepes, 0.025 EGTA, 2 Mg-ATP, 0.2 Na_2-GTP, and 10 Na_2-phosphocreatine, pH 7.2 to 7.3, 285 to 290 mOsm/kg.

We identified virus-expressing cells using scanning-disk confocal microscopy (Olympus FV1000). We used differential interference contrast optics to identify and record from CeL neurons. We used an Axopatch 200B amplifier (Molecular Devices) and Axograph X software (Axograph Scientific) to record and collect the data, which we filtered at 10 kHz and digitized at 4 to 20 kHz. We monitored series resistance (R_s) and input resistance (R_{in}) with injection of hyperpolarizing current (20 pA, 500 ms); we excluded data if these parameters changed >20% during data acquisition. We measured repetitive firing using depolarizing current steps (800-ms duration, 50 to 450 pA, 20-pA increments for shPKCδ experiment, 800-ms duration, 50 to 190 pA, 20-pA increments for shSOM experiment).

Self-Administration Chambers. We combined a standard Med Associates self-administration chamber with a custom-made social-partner chamber separated by a guillotine door. Each chamber had a discriminative stimulus on the right panel (white houselight) that signaled the availability of the social reward-paired lever and a discriminative stimulus on the left panel (red lens) that signaled the availability of the drug-paired lever located on the left side. There was also an inactive lever on the left side. A white cue light was located above the drug-paired lever and a tone cue above the social-paired lever (12–14).

Procedures.

Social self-administration. We trained rats to self-administer a social partner during daily 40-min sessions (20 trials per session, 60 s) using a discrete trial design. The trials started with the illumination of the social-paired houselight followed 10 s later with insertion of the social-paired active lever; we allowed the resident rat a maximum of 60 s to press the lever on a fixed-ratio-1 (FR1) reinforcement schedule before it retracted and the houselight turned off. Successful lever presses caused the retraction of the active lever, followed by a 20-s tone cue and opening of the guillotine door. The resident rat was subsequently allowed to interact with the social partner for 60 s until the houselight turned off, at which point the guillotine door closed and we manually replaced both rats in their appropriate chambers. We recorded the number of successful trials and inactive lever presses (12–14).

Drug self-administration. We trained rats to self-administer methamphetamine during six 1-h sessions that were separated by 10-min off periods under an FR1 20-s timeout reinforcement schedule. We limited the number of infusions to 15/h. The sessions began with the presentation of the red light and 10 s later with insertion of the drug-paired active lever; the red light served as a discriminative stimulus for drug availability. At the end of each 1-h session, the red light was turned off, and the active lever was retracted (48).

Voluntary abstinence. We conducted the discrete choice sessions during the voluntary abstinence using the same parameters used during social and methamphetamine self-administration training. We allowed the rats to choose between the social- and drug-paired levers in a discrete trial choice procedure for 10 sessions over 14 d. We divided each 120-min choice session into 15 discrete trials that were separated by 8 min (12–14). Each trial began with presentations of the discriminative stimuli for social interaction and methamphetamine, followed 10 s later by insertion of the levers paired with the rewards. Rats could then select one of the two levers. If rats responded within 6 min, they only received the reward associated with the selected lever. Each reward delivery was signaled by the social or drug-associated cue, retraction of both levers, and turning off the discriminative cues. If rats failed to respond on either active lever within 6 min, both levers were retracted, and the discriminative stimuli were turned off with no reward delivery.

Forced abstinence. After the completion of the training phase, we kept the rats in their homecage and handled them 3–4 times per week (48).

Relapse tests. The relapse test in the presence of drug cues consisted of 30- or 90-min sessions. The sessions began with the presentation of the methamphetamine-paired discriminative cue, followed 10 s later by insertion of the methamphetamine-paired lever. Active lever presses during testing, the operational measure of drug seeking in incubation of craving and relapse studies (17, 49), caused contingent presentations of the light cue previously paired with methamphetamine infusions but not methamphetamine.

Specific Experiments.

Experiment 1A: shPKCδ validation.

Immunohistochemistry. We injected six rats with $shCtrl_{PKCδ}$ into the CeL of one hemisphere and shPKCδ into the other hemisphere (0.75 μL; counterbalanced) either 2 or 4 wk before novel context exposure. We combined the 2- and 4-wk data because we observed similar viral expression. On test day, we placed the rats into a novel context (spherical container with fresh bedding and colorful toys) to induce Fos expression and 90 min later anesthetized the rats with isoflurane, perfused them, and extracted their brains for subsequent immunohistochemistry assays.

Electrophysiology. We performed whole-cell current clamp recordings in CeL and examined the effect of the viruses ($shCtrl_{PKCδ}$ $n = 7$ cells/5 rats; shPKCδ $n = 9$ cells/5 rats) on intrinsic properties.

Experiment 1B: shSOM validation.

Immunohistochemistry. We injected two groups of rats ($n = 5$ per group) bilaterally with $shCtrl_{SOM}$ (0.375 μL) or shSOM into the CeL 4 wk before novel context exposure. We selected the 4-wk time point period based on our data with the shPKCδ. On test day, we placed the rats into the novel context to induce Fos expression and 90 min later deeply anesthetized the rats, perfused them, and extracted their brains.

Electrophysiology. We performed whole-cell current clamp recordings in CeL and examined the effect of the viruses ($shCtrl_{SOM}$ $n = 9$ cells/5 rats; shSOM $n = 6$ cells/5 rats) on intrinsic properties.

Experiment 2: Effect of shPKCδ on incubation of methamphetamine craving after voluntary abstinence.

Training. We first trained rats to self-administer social interaction (6 sessions, 20 trials per session) and then trained them to self-administer methamphetamine (12 sessions, 6 h per session; 0.1 mg/kg/infusion).

Voluntary abstinence. We determined social interaction versus methamphetamine preference for 10 d over 14 d, preceding the abstinence day 15 relapse test.

Relapse tests. We tested the rats for methamphetamine seeking under extinction conditions on abstinence days 1 and 15. The duration of the test session was 30 min on abstinence day 1 to minimize carryover effect of extinction learning, which may decrease drug seeking on day 15 testing. Immediately after the 90-min day 15 relapse test, we anesthetized the rats and perfused them. We extracted the brains and processed the tissue for viral expression and for Fos expression, PKCδ and SOM protein levels, and double-labeled expression in CeL and CeM.

Experiment 3: Effect of shSOM on incubation of methamphetamine craving after forced abstinence.

Training. We trained rats to self-administer methamphetamine (12 sessions, 6 h per session; 0.1 mg/kg/infusion).

Forced abstinence. After the day 1 relapse test, we returned the rats to their homecage for 14 d and handled them three to four times per week.

Relapse tests. The tests were identical to those reported in experiment 2.

Statistical Analysis. We used factorial ANOVAs and *t* tests using Statistical Package for the Social Sciences (SPSS) (IBM, version 25, GLM procedure). We followed significant main and interaction effects ($P < 0.05$, two-tailed) with post hoc tests (Fisher PLSD). We only report significant effects critical for data interpretation and indicate results of post hoc analyses in the figures. For choice data, we performed the statistical analyses on preference score (number of social rewards/[number of social reward + number of methamphetamine infusions]). In *SI Appendix*, Table S1, we provide a complete report of the statistical results. No statistical methods were used to predetermine sample sizes, and our sample sizes are based on our previous studies (12, 13). Data distribution was assumed to be normal, but this was not formally tested.

Data Availability. Materials, datasets, and protocols are available upon request from M.V. or Y.S.

ACKNOWLEDGMENTS. We thank Michelle Zhang for her help during the experiments. We acknowledge the Genetic Engineering and Viral Vector Core at NIDA. The research was supported by the Intramural Research Program of NIDA, a fellowship from the NIH Center on Compulsive Behaviors (M.V.), National Institute of Alcohol Abuse and Alcoholism grant AA026075 (R.O.M.), and National Alliance for Research on Schizophrenia & Depression (NARSAD) Distinguished Investigator Grant Award (Y.S.).

1. M. Heilig, D. H. Epstein, M. A. Nader, Y. Shaham, Time to connect: Bringing social context into addiction neuroscience. *Nat. Rev. Neurosci.* **17**, 592–599 (2016).
2. G. A. Marlatt, J. S. Baer, D. M. Donovan, D. R. Kivlahan, Addictive behaviors: Etiology and treatment. *Annu. Rev. Psychol.* **39**, 223–252 (1988).
3. N. H. Azrin, Improvements in the community-reinforcement approach to alcoholism. *Behav. Res. Ther.* **14**, 339–348 (1976).
4. K. Dunn *et al.*, Employment-based reinforcement of adherence to oral naltrexone in unemployed injection drug users: 12-month outcomes. *Psychol. Addict. Behav.* **29**, 270–276 (2015).

NEUROSCIENCE

Downloaded by guest on November 3, 2020

5. A. Wikler, Dynamics of drug dependence. Implications of a conditioning theory for research and treatment. *Arch. Gen. Psychiatry* **28**, 611–616 (1973).
6. C. R. Schuster, T. Thompson, Self administration of and behavioral dependence on drugs. *Annu. Rev. Pharmacol.* **9**, 483–502 (1969).
7. C. P. O'Brien, Experimental analysis of conditioning factors in human narcotic addiction. *Pharmacol. Rev.* **27**, 533–543 (1975).
8. G. M. Hunt, N. H. Azrin, A community-reinforcement approach to alcoholism. *Behav. Res. Ther.* **11**, 91–104 (1973).
9. K. Silverman, A. DeFulio, S. O. Sigurdsson, Maintenance of reinforcement to address the chronic nature of drug addiction. *Prev. Med.* **55** (suppl.), S46–S53 (2012).
10. W. M. Aklin *et al*., A therapeutic workplace for the long-term treatment of drug addiction and unemployment: Eight-year outcomes of a social business intervention. *J. Subst. Abuse Treat.* **47**, 329–338 (2014).
11. S. H. Ahmed, Trying to make sense of rodents' drug choice behavior. *Prog. Neuropsychopharmacol. Biol. Psychiatry* **87**, 3–10 (2018).
12. M. Venniro *et al*., Volitional social interaction prevents drug addiction in rat models. *Nat. Neurosci.* **21**, 1520–1529 (2018).
13. M. Venniro, T. I. Russell, M. Zhang, Y. Shaham, Operant social reward decreases incubation of heroin craving in male and female rats. *Biol. Psychiatry* **86**, 848–856 (2019).
14. M. Venniro, Y. Shaham, An operant social self-administration and choice model in rats. *Nat. Protoc.*, 10.1038/s41596-020-0296-6.
15. V. Deroche-Gamonet, D. Belin, P. V. Piazza, Evidence for addiction-like behavior in the rat. *Science* **305**, 1014–1017 (2004).
16. J. W. Grimm, B. T. Hope, R. A. Wise, Y. Shaham, Neuroadaptation. Incubation of cocaine craving after withdrawal. *Nature* **412**, 141–142 (2001).
17. C. L. Pickens *et al*., Neurobiology of the incubation of drug craving. *Trends Neurosci.* **34**, 411–420 (2011).
18. M. E. Wolf, Synaptic mechanisms underlying persistent cocaine craving. *Nat. Rev. Neurosci.* **17**, 351–365 (2016).
19. J. Gründemann, A. Lüthi, Ensemble coding in amygdala circuits for associative learning. *Curr. Opin. Neurobiol.* **35**, 200–206 (2015).
20. S. Ciocchi *et al*., Encoding of conditioned fear in central amygdala inhibitory circuits. *Nature* **468**, 277–282 (2010).
21. W. Haubensak *et al*., Genetic dissection of an amygdala microcircuit that gates conditioned fear. *Nature* **468**, 270–276 (2010).
22. P. Tovote *et al*., Midbrain circuits for defensive behaviour. *Nature* **534**, 206–212 (2016).
23. K. Yu *et al*., The central amygdala controls learning in the lateral amygdala. *Nat. Neurosci.* **20**, 1680–1685 (2017).
24. H. Li *et al*., Experience-dependent modification of a central amygdala fear circuit. *Nat. Neurosci.* **16**, 332–339 (2013).
25. K. Yu, P. Garcia da Silva, D. F. Albeanu, B. Li, Central amygdala somatostatin neurons gate passive and active defensive behaviors. *J. Neurosci.* **36**, 6488–6496 (2016).
26. M. A. Penzo, V. Robert, B. Li, Fear conditioning potentiates synaptic transmission onto long-range projection neurons in the lateral subdivision of central amygdala. *J. Neurosci.* **34**, 2432–2437 (2014).
27. S. Ahrens *et al*., A central extended amygdala circuit that modulates anxiety. *J. Neurosci.* **38**, 5567–5583 (2018).
28. J. Kim, X. Zhang, S. Muralidhar, S. A. LeBlanc, S. Tonegawa, Basolateral to central amygdala neural circuits for appetitive behaviors. *Neuron* **93**, 1464–1479.e5 (2017).
29. T. D. Wilson *et al*., Dual and opposing functions of the central amygdala in the modulation of pain. *Cell Rep.* **29**, 332–346.e5 (2019).
30. X. Li, T. Zeric, S. Kambhampati, J. M. Bossert, Y. Shaham, The central amygdala nucleus is critical for incubation of methamphetamine craving. *Neuropsychopharmacology* **40**, 1297–1306 (2015).
31. D. Funk *et al*., Role of central amygdala neuronal ensembles in incubation of nicotine craving. *J. Neurosci.* **36**, 8612–8623 (2016).
32. M. Venniro *et al*., The anterior insular cortex→central amygdala glutamatergic pathway is critical to relapse after contingency management. *Neuron* **96**, 414–427.e8 (2017).
33. M. J. Robinson, S. M. Warlow, K. C. Berridge, Optogenetic excitation of central amygdala amplifies and narrows incentive motivation to pursue one reward above another. *J. Neurosci.* **34**, 16567–16580 (2014).
34. S. M. Warlow, M. J. F. Robinson, K. C. Berridge, Optogenetic central amygdala stimulation intensifies and narrows motivation for cocaine. *J. Neurosci.* **37**, 8330–8348 (2017).
35. E. A. Stein *et al*., Nicotine-induced limbic cortical activation in the human brain: A functional MRI study. *Am. J. Psychiatry* **155**, 1009–1015 (1998).
36. S. Grant *et al*., Activation of memory circuits during cue-elicited cocaine craving. *Proc. Natl. Acad. Sci. U.S.A.* **93**, 12040–12045 (1996).
37. M. J. McHugh *et al*., Cortico-amygdala coupling as a marker of early relapse risk in cocaine-addicted individuals. *Front. Psychiatry* **5**, 16 (2014).
38. M. T. Sutherland *et al*., Down-regulation of amygdala and insula functional circuits by varenicline and nicotine in abstinent cigarette smokers. *Biol. Psychiatry* **74**, 538–546 (2013).
39. National Research Council, *Guide for the Care and Use of Laboratory Animals* (National Academies Press, Washington, DC, ed. 8, 2011).
40. G. Paxinos, C. Watson, *The Rat Brain in Stereotaxic Coordinates* (Academic Press, San Diego, CA, ed. 6, 2008).
41. D. A. Rubinson *et al*., A lentivirus-based system to functionally silence genes in primary mammalian cells, stem cells and transgenic mice by RNA interference. *Nat. Genet.* **33**, 401–406 (2003). Correction in: *Nat. Genet.* **39**, 803 (2007).
42. A. W. Lasek, P. H. Janak, L. He, J. L. Whistler, U. Heberlein, Downregulation of mu opioid receptor by RNA interference in the ventral tegmental area reduces ethanol consumption in mice. *Genes Brain Behav.* **6**, 728–735 (2007).
43. X. Yu *et al*., Wakefulness is governed by GABA and histamine cotransmission. *Neuron* **87**, 164–178 (2015).
44. M. B. Pomrenze *et al*., Dissecting the roles of GABA and neuropeptides from rat central amygdala CRF neurons in anxiety and fear learning. *Cell Rep.* **29**, 13–21 e14 (2019).
45. X. Li *et al*., Role of dorsal striatum histone deacetylase 5 in incubation of methamphetamine craving. *Biol. Psychiatry* **84**, 213–222 (2018).
46. D. B. Howard, B. K. Harvey, Assaying the stability and inactivation of AAV serotype 1 vectors. *Hum. Gene Ther. Methods* **28**, 39–48 (2017).
47. D. Caprioli *et al*., Role of dorsomedial striatum neuronal ensembles in incubation of methamphetamine craving after voluntary abstinence. *J. Neurosci.* **37**, 1014–1027 (2017).
48. D. Caprioli *et al*., Effect of the novel positive allosteric modulator of metabotropic glutamate receptor 2 AZD8529 on incubation of methamphetamine craving after prolonged voluntary abstinence in a rat model. *Biol. Psychiatry* **78**, 463–473 (2015).
49. M. Venniro, D. Caprioli, Y. Shaham, Animal models of drug relapse and craving: From drug priming-induced reinstatement to incubation of craving after voluntary abstinence. *Prog. Brain Res.* **224**, 25–52 (2016).

Downloaded by guest on November 3, 2020